iScience

CellPress
OPEN ACCESS

Article

Fatty acid metabolism decreased while sexual selection increased in brown rats spreading south

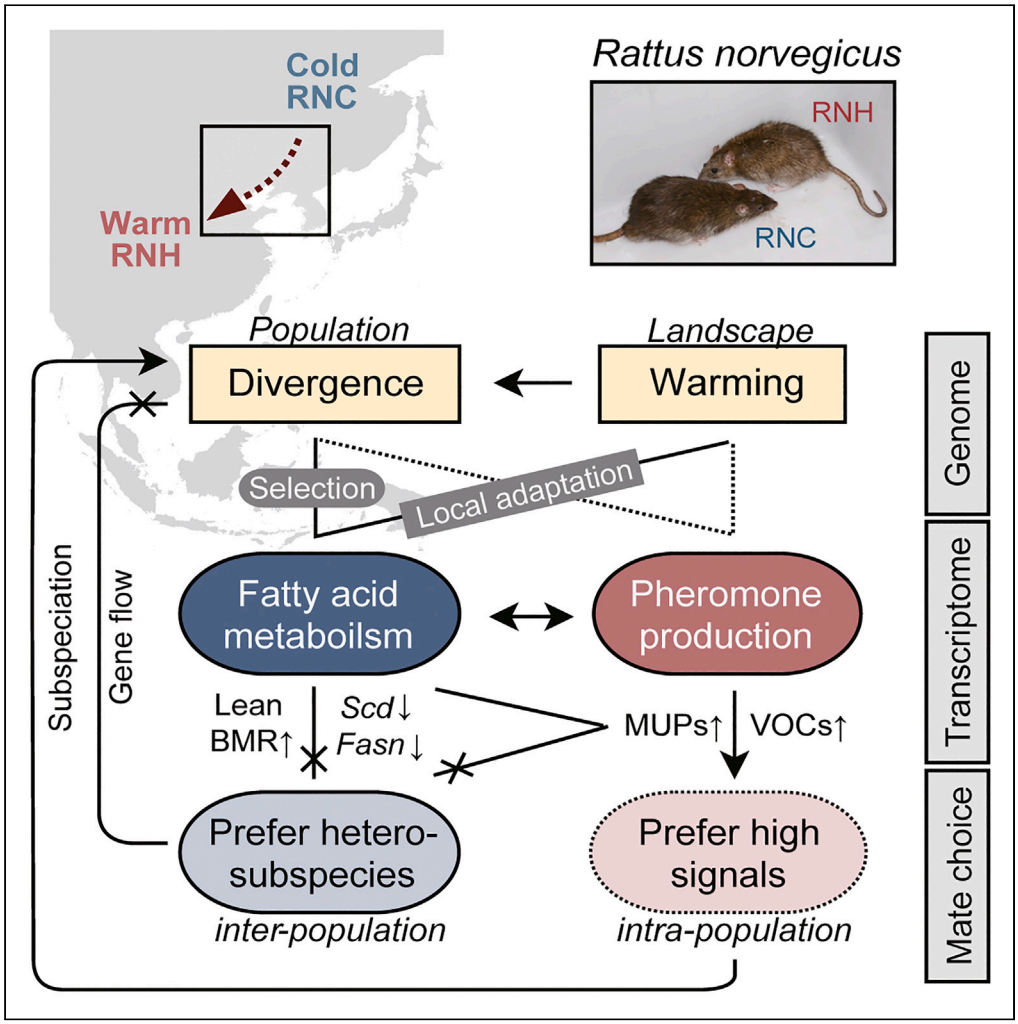

Yao-Hua Zhang, Lei Zhao, Ming-Yu Zhang, Rui-Dong Cao, Guan-Mei Hou, Hua-Jing Teng, Jian-Xu Zhang

zhangyh.eco@outlook.com (Y.-H.Z.)
zhangjx.rat@outlook.com (J.-X.Z.)

Highlights

RNH spread from cold Northeast China to warm North China

RNH and its source population RNC diverged in phenotype and genomic patterns

Temperature was the main environmental factor driving divergence and adaptation

Decreased fat synthesis and strengthened pheromone signals facilitated invasion success

Zhang et al., iScience 26, 107742
October 20, 2023
https://doi.org/10.1016/j.isci.2023.107742

iScience

CellPress
OPEN ACCESS

Article

Fatty acid metabolism decreased while sexual selection increased in brown rats spreading south

Yao-Hua Zhang,[1,*] Lei Zhao,[1,2] Ming-Yu Zhang,[1,2] Rui-Dong Cao,[1,2] Guan-Mei Hou,[1,2] Hua-Jing Teng,[3] and Jian-Xu Zhang[1,2,4,*]

SUMMARY

For mammals that originate in the cold north, adapting to warmer environments is crucial for southwards invasion. The brown rat (*Rattus norvegicus*) originated in Northeast China and has become a global pest. *R. n. humiliatus* (RNH) spread from the northeast, where *R. n. caraco* (RNC) lives, to North China and diverged to form a subspecies. Genomic analyses revealed that subspecies differentiation was promoted by temperature but impeded by gene flow and that genes related to fatty acid metabolism were under the strongest selection. Transcriptome analyses revealed downregulated hepatic genes related to fatty acid metabolism and upregulated those related to pheromones in RNH vs. RNC. Similar patterns were observed in relation to cold/warm acclimation. RNH preferred mates with stronger pheromone signals intra-populationally and more genetic divergence inter-populationally. We concluded that RNH experienced reduced fat utilization and increased pheromone-mediated sexual selection during its invasion from the cold north to warm south.

INTRODUCTION

Invasive rats (*Rattus* spp.) are among the most widespread and damaging invasive species.[1,2] Among the numerous species within the genus *Rattus*, three species—the brown rat (*Rattus norvegicus*), the black or roof rat (*Rattus rattus*), and the Asian house rat (*Rattus tanezumi*)—are global commensals and are often dispersed by human activities.[3,4] In contrast to the other commensal *Rattus* species that originated in southern Asia, brown rats are thought to have originated in the north, especially in Heilongjiang Province in the most northeastern part of China and Mongolia, and have high tolerance to cold environments.[5] It is the most recent invader of the invasive *Rattus* species, possibly due to its northern origin, and mostly spread southwards into warmer areas: it first spread to North, East, Central, and South China and then expanded to Southeast Asia, the Middle East and Europe, western Africa, eastern North America, western North America, South America, New Zealand, and Australia in the last thousand years.[2,5–10] Especially in Europe, brown rats outcompete and largely displace historically introduced black rats (*R. rattus*), becoming the dominant rat species.[2,5,10,11] As the most destructive pest, the brown rat causes considerable economic costs related to crops and infrastructure, spreads zoonotic diseases, and even contributes to the extinctions or declines of flightless invertebrates, ground-dwelling reptiles, land birds, and burrowing seabirds.[1,3,12,13] For instance, on Hawadax Island (previously known as Rat Island) in the Aleutian Islands, invasive brown rats disrupted the ecosystem for two centuries until rat eradication in 2008, and the biota recovered and now resembles that of nearby rat-free islands, which serves as an exemplary case of ecosystem recovery.[12]

Invasion success largely depends on local adaptation that enables invaders to expand their ranges and occupy a broader array of habitats.[14] Local adaptation is associated with divergent natural selection, including ecological selection and sexual selection.[15–18] Adaptation to changing climatic conditions can influence evolutionary dynamics during range expansion.[19–21] For example, precipitation shaped genomic differentiation, and areas of elevated genome–environment association overlapped with areas of rapid ecological transition in Misonne's soft-furred mice (*Praomys misonnei*).[22] Temperature is a key climatic factor and selection pressure driving local adaptation and even speciation.[23–26] Temperatures are usually associated with latitudes, and it is important to investigate adaptation and differentiation along latitudinal gradients.[23,27,28] Mammals have evolved the ability to maintain a stable body temperature by regulating metabolic processes, and their southwards-expanded populations must adapt to warmer regions to survive and colonize successfully.[18,19,29–33]

[1]State Key Laboratory of Integrated Management of Pest Insects and Rodents in Agriculture, Institute of Zoology, Chinese Academy of Sciences, Beichen West Road 1-5, Chaoyang District, Beijing 100101, China
[2]CAS Center for Excellence in Biotic Interactions, University of Chinese Academy of Sciences, Beijing 100049, China
[3]Key Laboratory of Carcinogenesis and Translational Research (Ministry of Education/Beijing), Department of Radiation Oncology, Peking University Cancer Hospital & Institute, Beijing 100142, China
[4]Lead contact
*Correspondence: zhangyh.eco@outlook.com (Y.-H.Z.), zhangjx.rat@outlook.com (J.-X.Z.)
https://doi.org/10.1016/j.isci.2023.107742

Populations inhabiting different geographic areas show marked phenotypic and genetic differentiation and a wide range of adaptations.[5,6,34] Invading populations are often differentiated in ecologically important traits, which promotes successful establishment.[14] They may have higher metabolic rates and a faster pace of life.[35] They are also presumed to optimize their mating-related traits as well as survival-related traits.[15,16,36] The expression of sexual traits and sex-biased genes is condition-dependent to meet the demands of the local environment; meanwhile, movement into new environments can strengthen sexual selection and sexual traits.[15,16,36–38] In mammals, pheromones are composed of urine-borne volatile organic compounds (VOCs) and major urinary proteins (MUPs); these molecules, which are mainly produced in the liver, play a role not only in sexual selection but also in metabolism.[39–41] For instance, in rats and mice, the VOC 2-heptanone is produced during fatty acid metabolism, and MUPs can suppress both gluconeogenesis and lipogenesis.[42–45] Hepatic lipid metabolism can be affected by ambient temperature; specifically, stearoyl-CoA desaturase (*Scd*), a key enzyme for lipid synthesis and fat synthesis, is strikingly increased in cold environments.[46–48]

As one of the most harmful invasive species, brown rats are increasingly studied in urban and global contexts for their population structure and spread; however, little is known about their local adaptation in the southwards expansion of the geographical range.[5,49–54] In China, the brown rat is morphologically divided into four subspecies or geographic populations, namely, the origin population *R. n. caraco* (RNC) and the three invaded populations *R. n. humiliatus* (RNH), *R. n. soccer*, and *R. n. norvegicus*, of which the distributions are largely associated with latitudinal temperature gradients.[6,50,55–58] RNC lives in the native range of the middle and cold temperate zones in Northeast China; RNH, which is derived from RNC, has colonized the adjacent warmer regions in the warm temperature zone (more than 10°C warmer than Northeast China in winter) and differentiated as a subspecies, providing a unique opportunity to investigate how invaders adapt to warmer ambient conditions.[5,6] Compared to RNC, RNH has a lighter coat, a smaller and leaner body, higher levels of 2-heptanone and MUP, and a unique pheromone-mediated mate choice strategy, suggesting that these traits might be interconnected and associated with local/warm-climate adaptation.[6,15,16,36,37,40,55,56,59–62] Although RNH has obviously diverged from its source population RNC, its genomic patterns and adaptation remain unclear. Moreover, whether the strengthened pheromone signals and pheromone-mediated mate choice are related to metabolism and warmth and how these associations contribute to adaptation and subspeciation deserve investigation.

Here, we analyzed the whole-genome sequences (WGSs) of 48 rats sampled along a 1100 km transect within the distribution ranges of RNC and RNH and explored their genomic adaptations to environmental changes across latitudes. We further compared the hepatic transcriptomes of RNH vs. RNC and temperature-acclimated rats to explore the physiological changes in gene expression levels in response to ambient temperature changes. We also examined cross-mating preferences and cross-breeding success between RNH rats and RNC rats and inferred their potential effects on subspecies differentiation.

RESULTS

Population structure, genomic divergence and gene flow

The 48 *R. norvegicus* samples analyzed in the current study extended from Harbin (HB, the center of the RNC range) to Beijing (BJ, the center of the RNH range) in northern China (Figure 1A; Table S1). After stringent quality control, we identified a total of 27.59 million single nucleotide polymorphisms (SNPs), used a linkage disequilibrium (LD)-pruned subset of 3.36 million SNPs, and conducted both model-based and model-free methods to infer population structure. ADMIXTURE v1.3[63] analysis revealed that K = 2 was the most likely number of genetic clusters. In principle component analysis (PCA), spatial PCA (sPCA), and TESS analysis,[64] the spatial arrangement of samples was consistent with their geographic locations, where samples were divided into two parts, and the border region was located between Linghai (LH) and Xingcheng (XC) (Figures 1A–1D, S1, and S2). Similarly, in fineSTRUCTURE v4.0.1 analysis[65] that explored the population structure in more detail, the samples were clustered by geographic origin: the RNH clade (consisting of the RNH1 subclade and the RNH2 subclade) ranged from BJ to XC and was differentiated from the RNC clade (consisting of subclades of RNC1 and RNC2) that ranged from LH to HB. Individuals from the same clade/subclade had higher coancestry than those from different clades/subclades, except for the LH and XC samples, indicating intense gene flow (Figure 1E). TREEMIX v1.12[66] predicted gene flow from RNC to the outgroup and from RNH2 to RNC2 (Figures 1F and S3).

Demographic histories of the two subspecies

To reconstruct the demographic history of the two subspecies, we performed both model-free and model-based demographic inference. The divergence time of RNC and RNH was ~1.37 kya, as inferred by the generalized phylogenetic coalescent sampler (G-PhoCS) v1.2.3[67] (Table S2). To infer the changes in effective population size (Ne) over time, we additionally performed site frequency spectrum (SFS)-based methods with Stairway Plot v2[68] and fastsimcoal2 v2.6.[69] Stairway Plot revealed that the two subspecies declined from 30 to 40 kya and have had different demographic histories since ~1 kya. RNC experienced a bottleneck ~300–500 years ago (Ne = 2.7 k), while RNH underwent a steady decline. The recent Ne values of RNH and RNC were ~10 k (Figure 1G). We fit five models by fastsimcol2: isolation-only (IO), isolation-with-migration (IM), IM-and-bottleneck (IMB), isolation-with-secondary contact (SC) and IMB-with-secondary contact (IMBSC) models. The best-supported model was the IMB model (Table S3). RNH and RNC diverged from an ancestral population (Ne = 211924) into two populations (Ne: RNH, initial = 50555, present = 48380; RNC, initial = 221292, present = 117113, bottleneck = 6220), and the per-generation migration rates from RNH to RNC and from RNC to RNH were 1.09×10^{-5} and 1.22×10^{-7}, respectively (Figure 1H; Table S3).

Environmental factors influencing genetic variation

To explore the relationship between environmental variation and genetic variance, we downloaded climatic data from public databases. First, we related the genetic distances between all pairs of sampling sites to between-site landscape factors. We evaluated the following

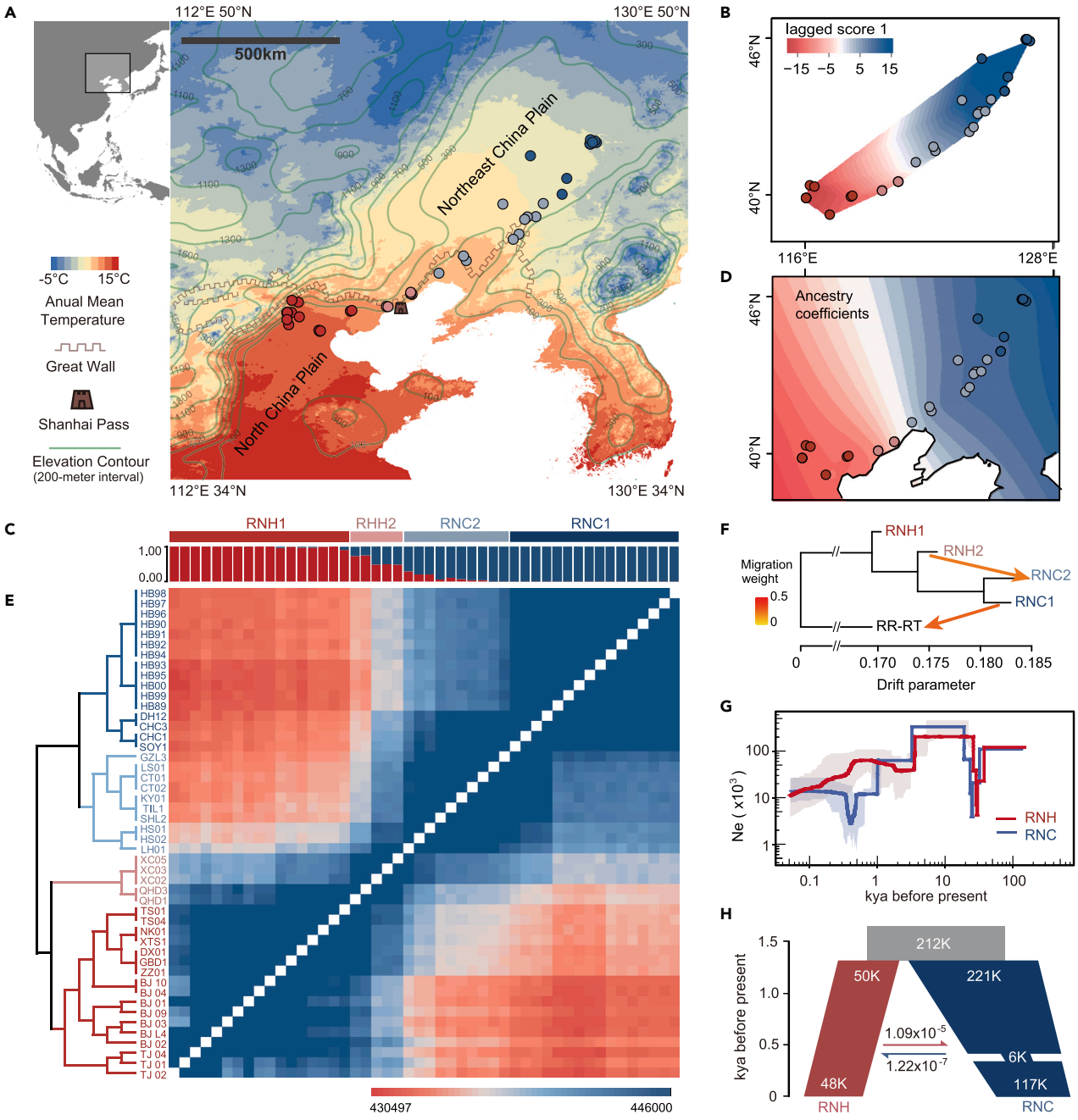

Figure 1. Genomic divergence between RNC and RNH subspecies

(A) Forty-eight *R. norvegicus* samples spanning from Harbin to Beijing were analyzed in this study.

(B) Interpolated map of individual lagged PC 1 scores from sPCA.

(C) Cluster analysis computed by TESS.

(D) Admixture analysis performed using ADMIXTURE.

(E) Coancestry heatmap from fineSTRUCTURE analysis, where red and blue denote lower and higher coancestry levels, respectively.

(F) TREEMIX analysis with four migration edges.

(G) Estimates of effective population size (Ne) over time obtained using a stairway plot with ribbons showing the 95% confidence intervals.

(H) Estimates of Ne and migration rates obtained using fastsimcol2; the deme size corresponds to two times the number of individuals, and migration occurs forwards in time. Individuals were classified into four groups based on the results of fineSTRUCTURE and geographic locations. RNH1, RNH2, RNC1 and RNC2 are represented by dark red, light red, dark blue and light blue dots, respectively, in panels (A-C). Detailed information on each sample is provided in Table S1.

Table 1. Mantel tests for the effects of IBD, IBB and IBE on genetic distance

	Distance	Barrier	Climate	Elevation	Population	Crop
Distance	0.761***	0.612***	0.189**	0.750***	0.750***	0.761***
Barrier	0.394***	0.656***	0.354***	0.654***	0.651***	0.650***
Climate	0.148***	0.586***	0.756***	0.746***	0.750***	0.757***
Elevation	0.010	0.178***	−0.042	0.190***	0.188***	0.191**
Population	0.134*	0.211**	0.187**	0.233**	0.235***	0.211**
Crop	0.132*	0.025	0.128*	0.124*	0.063	0.122*

The diagonal entries show the results of simple Mantel tests between genetic variance and the variables; the other cells show the results of partial Mantel tests between the genetic variance and the row variables, with the column variables controlled for (*p < 0.05, **p < 0.01, ***p < 0.001. The full results are provided in Table S8).

models: isolation-by-distance (IBD), isolation-by-environment (IBE), isolation-by-resistance (IBR), and isolation-by-barrier (IBB) models. Mantel and partial Mantel tests revealed significant effects of geography, climatic distance, human population density and mountain barriers on genetic variance (Figure S4; Table 1).

Second, we estimated the correlations between the genetic variance at each sampling site and local environmental conditions by redundancy analysis (RDA) and found that the full model and the first two constrained axes were significant (p = 0.001). RNH was differentiated from RNC along RDA1, whereas RDA2 separated the subpopulations from the core populations (Figure 2A). Annual mean temperature and human population density, independent of the other variables, were strong predictors of genotypic variation again (p = 0.001, Table S5). Moreover, SNPs correlated with annual mean temperature were mainly related to palmitoyl-CoA 9-desaturase activity and the monounsaturated fatty acid biosynthetic process, and the SNPs correlated with human population density were mainly related to immune responses (Figure 2B; Table S6).

Genomic regions and genes under selection

The median F_{ST} between RNC1 and RNH1 was 0.084 [0.050–0.128], and the cross-population extended haplotype homozygosity (XP-EHH) score was 0.6142 [0.2858–1.0848]. The genetic diversity (π) in RNH was 1.389×10^{-3} [0.991×10^{-3}–1.838×10^{-3}], that in RNC was 1.347×10^{-3} [0.949×10^{-3}–1.789×10^{-3}] ($p < 2.2 \times 10^{-16}$), and the lgπratio was 4.810×10^{-2} [2.201×10^{-2}–9.085×10^{-2}] (Figure 3A; Table S7). The outlier regions had significantly higher values for F_{ST} ($p < 2.2 \times 10^{-16}$), the XP-EHH score ($p < 2.2 \times 10^{-16}$) and lgπratio ($p < 2.2 \times 10^{-16}$) than the simulated dataset, suggesting that the differentiation of these regions cannot be attributed to demographic processes (Figure 3A; Table S7).

Combining F_{ST}, XP-EHH and $lg\pi_{ratio,}$ we identified 715 genes in outlier regions (Figure 3A; Table S8), which were enriched in the Gene Ontology (GO) terms palmitoyl-CoA 9-desaturase activity, monounsaturated fatty acid biosynthetic process, haptoglobin-hemoglobin complex and fibrinogen complex (Figure 3B). Specifically, candidate genes such as *Scd* and *Fasn* were related to fatty acid biosynthesis, and *Etfb* participated in fatty acid beta-oxidation. We also found genes of hemoglobin subunits that contribute to oxygen binding activity, and fibrinogen subunits related to blood coagulation and fibrin clot formation were putatively under selection (Figure 3; Table S8).

Genomic and geographic clines along the subspeciation continuum

We identified SNPs with fixed differences between the core populations and selected 103 SNPs more than 1 Mb apart as diagnostic markers for the two subspecies (Table S9). We estimated the frequency changes along the subspeciation continuum by geographic and genomic cline analysis in the R packages HZAR v0.2-5[70] and introgress v1.2.3,[71] respectively. The median cline width between XC and LH was 434.25 [280.91–555.33] km, and the cline center was 670.109 [583.90–770.16] km from the northeast end (Harbin) (Figure 4A). The cline widths were strongly correlated with the cline centers (*rho* = 0.722, p < 0.001), suggesting that the cline centers shifted to the northeast as cline widths increased. Specifically, the hemoglobin subunits were close to marker 1:175168059, which had a cline center of 863.37 km and a narrow cline width of 0.74 km (Tables S9, S10, and S11). The *Scd* gene was close to marker 1:271389636, which had a cline center of 573.77 km and a wide cline width of 585.65 km and deviated from neutral expectations (p = 0.040; Figure 4B; Tables S9 and S10).

Temperature acclimation and divergent hepatic transcriptomes between subspecies

We assessed differences in MUPs and hepatic gene expression between the two subspecies and between two groups of RNH male rats allowed to acclimate to 2°C and 23°C for five consecutive days. We detected 129 hepatic differentially expressed genes (DEGs) between RNH and RNC and 207 DEGs in the acclimation group. Similar changes were observed for subspecific DEGs and acclimation DEGs. For instance, RNH had significantly higher expression levels of MUP genes (ENSRNOG00000009273, ENSRNOG00000042543, ENSRNOG00000046529, ENSRNOG00000049727, ENSRNOG00000050117, and ENSRNOG00000050595) than RNC; in the 23°C-acclimated rats, genes related to negative regulation of endopeptidase activity had significantly higher expression levels than those in the 2°C-acclimated rats (Figure 5; Table S12). Correspondingly, MUP levels were significantly higher in RNH rats (6.37 ± 1.03) than in RNC rats (1.17 ± 0.17) ($T = 4.971$, p = 0.004, $N = 6$) and higher in 23°C-acclimated rats (6.38 ± 0.58) than in 2°C-acclimated rats (2.48 ± 0.10) ($T = 5.955$, p = 0.002, $N = 6$).

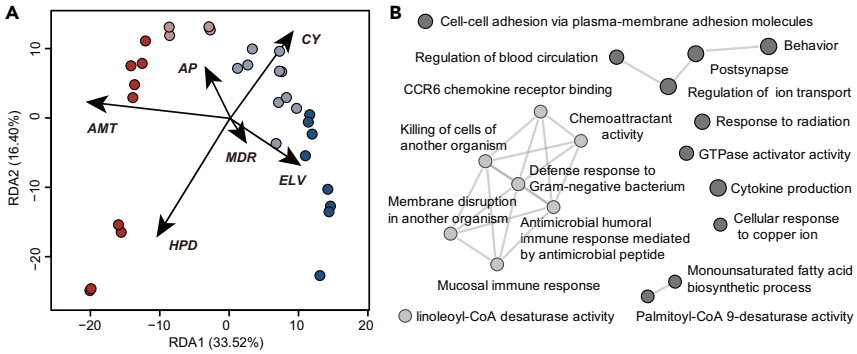

Figure 2. Local adaptation along the subspeciation continuum

(A) Redundancy analysis (RDA) assessing the genetic variation for each sample and local landscape factors for each sampling site. Landscape factors include annual mean temperature (AMT), annual precipitation (AP), mean diurnal range (MDR), human population density (HPD), crop yield (CY) and elevation (ELV). RNH1, RNH2, RNC1 and RNC2 samples are represented by dark red, light red, dark blue and light blue dots, respectively.

(B) Enrichment analysis of the genes associated with AMT (dark-grey dots) and HPD (light-grey dots).

Genes related to fatty acid metabolic processes had lower expression levels in both RNH and 23°C-acclimated rats, although the DEGs identified in the two experiments were different. In addition, the DEGs with lower expression in RNH were also related to cellular response to xenobiotic stimulus, negative regulation of epithelial cell apoptotic process, positive regulation of mitochondrial fission, regulation of macroautophagy, response to fatty acid, and negative regulation of secretion, and DEGs with lower expression in 2°C-acclimated rats were associated with response to glucocorticoid, acute-phase response, cellular response to peptide, regulation of small molecule metabolic process, organic acid transport, response to nutrient, hepatocyte differentiation, and positive regulation of phosphatidylinositol 3-kinase signaling (Figure 5).

Female mate choice between two subspecies of males

We examined female preferences for the two subspecies of males using a two-choice apparatus (Figure 6A).[61] Binary choice tests revealed that RNH females preferred RNC male scents to RNH male scents ($p = 0.028$, $Z = 2.201$, $N = 16$), and they also preferred live RNC males ($p = 0.049$, $Z = 1.965$, $N = 16$). RNC females preferred RNC male scents to RNH male scents ($p < 0.001$, $T = 5.803$, $N = 16$), whereas they responded equally to live RNC and RNH males ($p = 0.756$, $Z = 0.310$, $N = 16$). In the RNH female mating trios, 6 litters were sired by RNC males, 2 litters were sired by RNH males, and 5 litters had double paternity; RNC males sired more offspring than RNH males (RNC vs. RNH: 5.154 ± 3.555 vs. 2.077 ± 2.597, $Z = 1.890$, $p = 0.059$, $N = 13$, marginal but not significant). In the RNC female mating trios, 2 litters were sired by RNC males, 3 litters were sired by RNH males, and 8 litters had double paternity; there was no significant difference in the number of offspring sired by males between the two subspecies (RNC vs. RNH: 5.385 ± 4.011 vs. 4.385 ± 3.754, $T = 0.476$, $p = 0.643$, $N = 13$, Figure 6B).

DISCUSSION

Genomic differentiation between RNH and RNC and demographic histories

We found that an early dispersed population of RNH exhibited genome-wide divergence from the origin RNC population along the subspeciation continuum. The core populations of RNH1 and RNC1 were distributed around Beijing City in North China and Harbin City in Northeast China, respectively. The rats were clustered by geographic location and shared more genetic similarities and higher coancestry within clades; however, rats from LH and XC (belonging to the RNC2 and RNH2 clades, respectively) had high coancestry, indicating intense gene flow in this edge area. The gene flow was further supported by the migration events from RNH2 to RNC2 detected by TREEMIX. We observed asymmetric introgression where the centers of the wider clines shifted northeastward (RNH-to-RNC direction), and the median of the cline centers was located between LH and XC. Multiple analyses indicated that the subspecies boundary was in LH-XC in the Western Liaoning Corridor (185 km length, 8–15 km width), consistent with our previous findings based on microsatellite loci.[72] The transition populations RNH2 and RNC2, which extend 600 km from QHD to GZL and exhibit a clinal structure, may have arisen from a balance between dispersal and selection against hybrids, reflecting weak selection and gradual environmental gradients.[73]

We inferred that RNH diverged from RNC ~1.3 kya, and they experienced different demographic histories, where RNH showed a steady decline but RNC went through a bottleneck 300–500 years ago. The invasion of RNH approximately coincided with the human-mediated dispersal of brown rats from northern China to the south in AD 800–1550.[5] The bottleneck detected in RNC might be associated with the segregation and prohibitive policy of the "Willow Palisade", in which the Qing Dynasty government expelled agriculturalists in the northeast from the late 17th century to the mid-19th century.[74] In addition, human settlements and agriculture existed in China as far north as 47°N in the medieval warm period (MWP) and shifted southwards to 3–4° latitude (to Liaoning Province) in the Little Ice Age (LIA).[75] Temperature intricately interacts with agriculture and civilization to influence human migration, which indirectly influences the dispersal and differentiation of brown rats.[5,50]

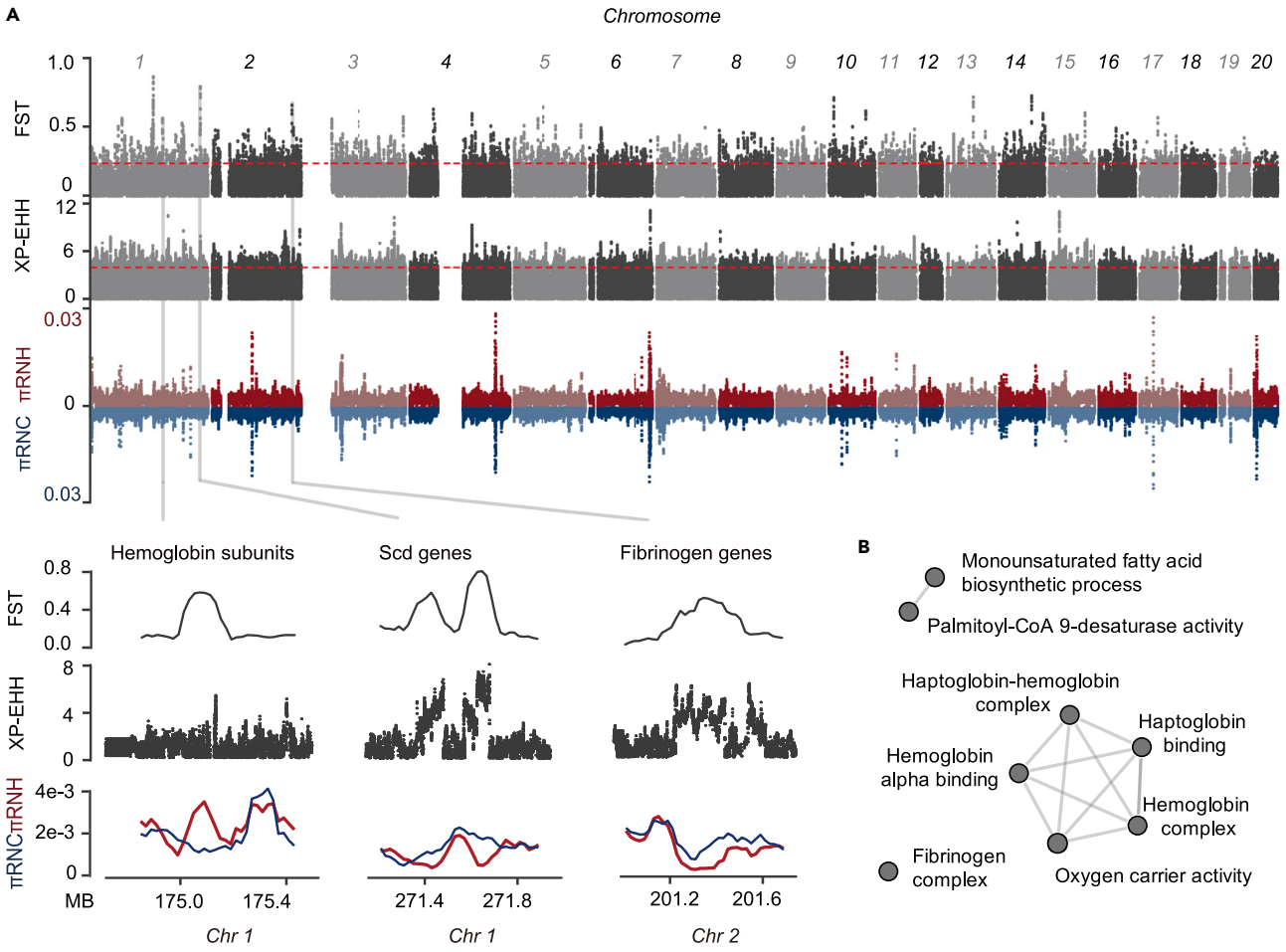

Figure 3. Genes under selection

(A) FST, XP-EHH and π values across the genome and in zoomed-in views of three outlier regions (hemoglobin subunits, *Scd* genes, and fibrinogen genes). The red dashed line represents the outlier threshold.

(B) Enrichment analysis of the 715 genes in the outlier regions shown in panel (A).

Temperature influenced differentiation and local adaptation

We found that geographic distance, climatic distance, human population density, and mountain barriers were important factors contributing to the differentiation of RNH from RNC. Environmental heterogeneity has been demonstrated to restrict the dispersal of brown rats and result in spatial isolation and genetic differentiation.[52–54] Human activities also affect genetic variation and adaptation in brown rats.[76] Since the effect of environmental resistance was not significant in our study, local selection pressure after colonization might play a greater role in shaping genetic variation patterns. We also observed that temperature and human population density were strongly correlated with genetic variance, similar to results reported in insects, birds and other mammals.[24,34,77–79] Therefore, climate temperature-mediated selection pressure may have promoted the adaptive genetic differentiation of brown rats observed in the current study.

We detected the adaptive loci for the two significant environmental predictors temperature and human population density and found that temperature was related to palmitoyl-CoA 9-desaturase activity and the monounsaturated fatty acid biosynthetic process. Meanwhile, these loci also displayed prominent selective sweep signals in FST, lgπratio, and XP-EHH analyses. Among the genes under the strongest selection, *Fasn* and *Scd* encode key enzymes that catalyze fatty acid synthesis, implying the importance of fatty acid metabolism in warm-climate adaptation in invasive RNH.[80] *Scd*, along with other genes associated with morphology and neuroendocrine and immune systems, showed broader clines that deviated from neutral expectations and thus could be important for survival and reproduction along the temperature gradient.[81]

The adaptive loci correlated with human population density were mainly associated with immune responses, such as defense response to Gram-negative bacterium, mucosal immune response, and antimicrobial humoral immune response mediated by antimicrobial peptide. Free-roaming domestic animals are reported to be interconnected with human density and pathogen prevalence.[82] As a commensal and invasive population, RNH have escaped many of the native diseases that RNC confronted, but they may also face novel pathogens in new habitats, resulting in corresponding changes to their immune systems. Like other invasive animals, RNH possibly rely on antibody-mediated

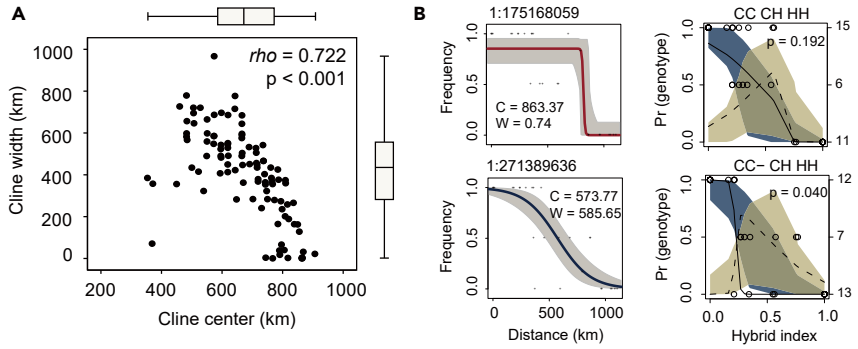

Figure 4. Geographic and genomic clines along the subspeciation continuum

(A) Correlations between cline centers and cline widths of the diagnostic markers.

(B) Cline analysis of two SNP markers (1:175168059, candidate genes: hemoglobin subunits; 1:271389636, candidate genes: *Scd* genes).

humoral immunity, which is less costly than systemic inflammatory responses, conserving resources for growth and reproduction.[83] Other molecules showing evidence of selective sweeps, such as hemoglobin subunits, fibrinogen subunits, and olfactory receptors, also contribute to the isolation and survival of the RNH subspecies, similar to results reported in house mice.[81,84]

Warm climate adaptation and changes in fatty acid metabolism

We found that the expression of some fatty acid metabolism genes was downregulated and that of MUP genes was upregulated in RNH compared with RNC, corresponding to higher MUP levels in the urine of RNH males than in that of RNC males.[61] Similarly, in temperature-acclimated rats, some fatty acid metabolism genes were downregulated in expression, and genes involved in the negative regulation of peptidase activity (reducing peptidase activity and protein breakdown and facilitating MUP accumulation) showed upregulated expression in warm-acclimated male rats compared with cold-acclimated male rats.

Specifically, *Scd* and *Fasn*, which are critical for fat synthesis and showed strong selective sweep signals, were significantly decreased in expression in RNH compared to RNC. This suggests that fatty acid biosynthesis was less active in RNH, in accordance with their leaner body and higher metabolic rates (unpublished data). Similarly, in mice, *Scd* knockout leads to lean and hypermetabolic phenotypes with increased energy expenditure, improved insulin sensitivity and decreased lipogenesis, while overexpression of *Scd* increases fatty acid synthesis in the liver, which can be induced by cold stimulation.[46–48,85,86] This finding supports the notion that invading populations may have high metabolic rates and exhibit 'fast' life histories, enabling them to rapidly and successfully colonize new biotopes.[35] Moreover, the expression of MUP genes strikingly increased in RNH. It has been exemplified in mice that MUPs are not only male ornaments but also important regulators of energy expenditure and metabolism, as well as inhibitors of both gluconeogenesis and lipogenesis.[43–45] VOCs such as 2-heptanone, generated in the process of fatty acid metabolism, were also significantly more abundant in RNH than in RNC.[47,61,87] Both VOCs and MUP pheromones might have interacted with metabolic processes and balanced the sexual selection traits with energy expenditure to cope

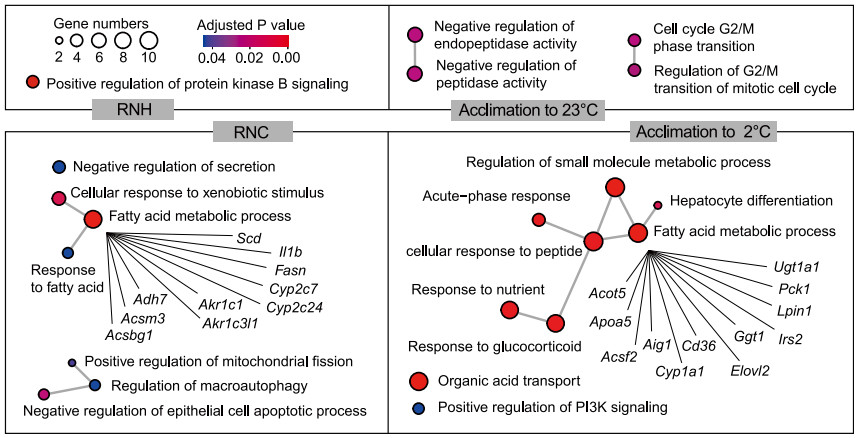

Figure 5. Functional enrichment analysis of the hepatic differentially expressed genes (DEGs) between RNH and RNC and between rats acclimated at 2°C and 23°C.

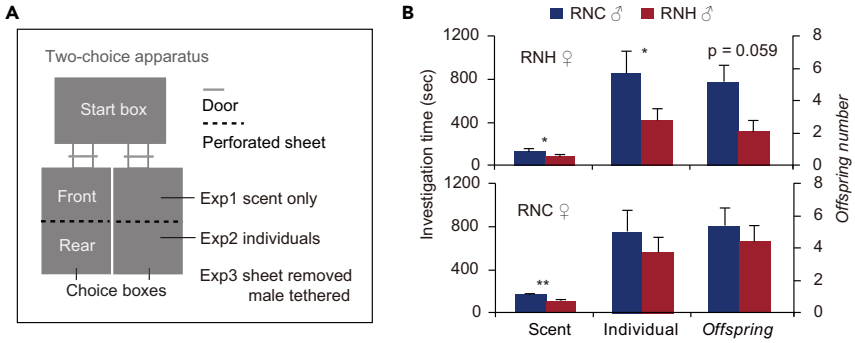

Figure 6. Mate choice and breeding success

(A) Two-choice apparatus for the mate choice test. In Exp1, male scents were placed in the front chambers; in Exp2, a male individual was placed in each of the rear chambers; and in Exp3, the sheets were removed, and males were loosely tethered in the choice boxes. Females were placed in the start box and allowed to freely investigate the front chambers in Exp1 and Exp2 and mate with males in Exp3.

(B) Females' investigation of male scent (Exp1), male individuals (Exp2) and offspring (Exp3) with the two subspecies of sires. Data are represented as mean ± SEM.

with the warm ambient conditions. Survival-related traits and mating-related traits can be condition-dependent and optimized to meet the demands of the local environment.[16,38]

Intra- and interpopulation mate choice and strengthened pheromone signals

We revealed that RNH diverged from the source population of RNC in genomic patterns, transcriptome profiles, pheromone signals and mate choice strategies. Moreover, both the intra- and interpopulation mate choices of RNH were different from those of RNC, which facilitated and impeded genomic divergence and contributed to subspeciation and local adaptation, respectively.

In the context of intrapopulation mate choice, RNH females prefer males with high-pheromone signals, while RNC females prefer dominant males despite low pheromone levels.[61,87] We have previously observed that RNH has significantly higher levels of VOCs and MUP pheromones than RNC[61](unpublished data). Here, we found that *Scd*, which participates in VOC pheromone production and is regulated by MUP pheromones, showed strong signals of selective sweeps and adaptation and was highly expressed in RNH. In addition, some genes participating in androgen metabolism and signaling pathways that potentially regulate pheromone production were also under positive selection.[39,40,42,61] Sexual selection may increase during expansions because of the fitness differential between mating with high- and low-quality males, especially in less favorable environments[16,37,38] When invading from cold areas into the adjacent warm-temperate zone, RNH underwent increases in sexually selected signals and relied heavily on mate choice to facilitate reproduction and rapidly and successfully colonize new habitats.

In the context of interpopulation mate choice, neither RNH nor RNC females displayed positive assortative mate choice. RNH females even showed a tendency for negative assortative mate choice, displaying a preference for and producing more offspring with the genetically divergent males of the RNC population despite low pheromone levels, coincident with the asymmetric introgression detected by cline analysis. Increasing heterozygosity and genetic diversity are particularly meaningful for improving the fitness of the brown rat, whose genetic diversity is much lower than that of house mice and other *Rattus* species, such as *R. tanezumi* and *R. nitidus*.[50,88,89] The trade-offs between male pheromones and other traits, such as coat color and body size, increased heterozygosity and impeded differentiation between RNH rats and RNC rats.[90,91]

Positive assortative mating promotes isolation; for example, in house mice (*Mus musculus*), *M. m. musculus* (*Mmm*) prefer their own subspecies over *M. m. domesticus* (*Mmd*), which facilitates subspeciation.[81,92] *Prdm9*, which encodes histone H3 lysine 4 trimethyltransferase and activates genes essential for meiosis, caused subspeciation of *Mmm* and *Mmd*.[93] Sterility genes induce abnormal spermatogenesis and consequent sterile hybrid males in subspecies of both house mice and European rabbit (*Oryctolagus cuniculus*).[93,94] We also found that some genes under selection might be associated with sperm function (*Ceacam4*, *Ppp2r3c*, *Pgk2*, *Septin12*, *Cct6a*, *Efcab2* and *Tssk6)* and androgen (*Andpro*, *Tiparp*, and *Akr1d1)*; however, there was no positive assortative mating or premating isolation, unlike the patterns in *Mmm* and *Mmd* mice.[92] The asymmetry of gene flow and introgression from RNH to RNC, which together with crossbreeding could hamper further divergence between RNH and RNC and thus maintain species integrity and cohesion, further supported the importance of temperature in the differentiation between RNH and RNC.

In conclusion, as the first descendant population dispersed from cold Northeast China to warm North China, RNH differentiated from its source population RNC in both phenotype and genomic pattern and diverged to form a subspecies. Temperature was the predominant environmental factor shaping its divergence and adaptation. To cope with the warm ambient environment, RNH evolved a leaner and smaller body, decreased fat synthesis and strengthened pheromone signals compared with those of RNC. Pheromones interacted with metabolic processes, and sexually selected traits were balanced with energy expenditure. The local adaptation in fatty acid metabolism, along with the associated pheromone signals and the signal-related mate choice strategies, facilitated invasion success.

Limitations of the study

In this study, we have illustrated the early stages of the global adventure of brown rats. Their steps have further moved on to other warmer areas, including the tropical zone and subtropical zone, and even back to cold areas. Other subspecies, such as *R. n. soccicus* and *R. n. norvegicus*, have also undergone selection, adaptation and divergence. How do fatty acid metabolism and pheromones function in more southerly and warmer areas and in other subspecies? Do they use other survival and/or reproduction strategies? Further research is needed to fully understand the global invasion of brown rats.

STAR★METHODS

Detailed methods are provided in the online version of this paper and include the following:

- KEY RESOURCES TABLE
- RESOURCE AVAILABILITY
  - Lead contact
  - Materials availability
  - Data and code availability
- EXPERIMENTAL MODEL AND STUDY PARTICIPANT DETAILS
  - Ethics approval
- METHOD DETAILS
  - Samples, DNA extraction, library preparation, and variant calling
  - Population structure analysis
  - Demographic history
  - Testing the influence of landscape on gene flow
  - Detection of loci under selection
  - Genomic and geographic cline analysis
  - Animals used for behavioral and physiological experiments
  - Temperature acclimation, hepatic MUP quantification and RNA-seq analysis
  - Behavioral tests of female preferences for male mates
- QUANTIFICATION AND STATISTICAL ANALYSIS

SUPPLEMENTAL INFORMATION

Supplemental information can be found online at https://doi.org/10.1016/j.isci.2023.107742.

ACKNOWLEDGMENTS

This work was supported by the National Natural Science Foundation of China (grant numbers 32070451 and 32090022) and the State Key Laboratory of Integrated Management of Pest Insects and Rodents (ChineseIPM 2102). We thank Jin-Hua Zhang for assistance in sample collection and behavioral tests.

AUTHOR CONTRIBUTIONS

Conceptualization, J.X.Z. and Y.H.Z.; Methodology, J.X.Z. and Y.H.Z.; Formal Analysis, Y.H.Z., J.X.Z., and L.Z.; Investigation, Y.H.Z., L.Z., M.Y.Z., R.D.C., G.M.H., and H.J.T; Resources, J.X.Z. and Y.H.Z.; Writing – Original Draft, J.X.Z. and Y.H.Z.; Writing – Review and Editing, J.X.Z. and Y.H.Z.; Supervision, J.X.Z.; Funding Acquisition, Y.H.Z.

Received: March 20, 2023
Revised: June 27, 2023
Accepted: August 24, 2023
Published: August 28, 2023

REFERENCES

1. Towns, D.R., Atkinson, I.A.E., and Daugherty, C.H. (2006). Have the harmful effects of introduced rats on islands been exaggerated? Biol. Invasions *8*, 863–891.
2. Aplin, K., and Ford, F. (2014). Murine rodents: late but highly successful invaders. In Invasion Biology and Ecological Theory: Insights from a Continent in Transformation, H.H.T. Prins and I.J. Gordon, eds. (Cambridge University Press), pp. 196–240.
3. Kosoy, M., Khlyap, L., Cosson, J.F., and Morand, S. (2015). Aboriginal and invasive rats of genus *Rattus* as hosts of infectious agents. Vector Borne Zoonotic Dis. *15*, 3–12.
4. Puckett, E.E., Orton, D., and Munshi-South, J. (2020). Commensal rats and humans: integrating rodent phylogeography and zooarchaeology to highlight connections between human societies. Bioessays *42*, e1900160.
5. Puckett, E.E., and Munshi-South, J. (2019). Brown rat demography reveals pre-commensal structure in eastern Asia before expansion into southeast Asia. Genome Res. *29*, 762–770.
6. Musser, G.G., and Carleton, M.D. (2005). Superfamily Muroidea. In Mammal species of the world a taxonomic and geographic reference, D.E. Wilson and D.M. Reeder,

eds. (Johns Hopkins University Press), pp. 894–1531.
7. Lack, J.B., Hamilton, M.J., Braun, J.K., Mares, M.A., and Van Den Bussche, R.A. (2013). Comparative phylogeography of invasive Rattus rattus and Rattus norvegicus in the U.S. reveals distinct colonization histories and dispersal. Biol. Invasions *15*, 1067–1087.
8. Puckett, E.E., Park, J., Combs, M., Blum, M.J., Bryant, J.E., Caccone, A., Costa, F., Deinum, E.E., Esther, A., Himsworth, C.G., et al. (2016). Global Population Divergence and Admixture of the Brown Rat (*Rattus norvegicus*). Proc. Royal Soc. B. *283*.
9. Russell, J.C., Robins, J.H., and Fewster, R.M. (2019). Phylogeography of invasive rats in New Zealand. Front. Ecol. Evol. *7*, 48.
10. Puckett, E.E., Magnussen, E., Khlyap, L.A., Strand, T.M., Lundkvist, Å., and Munshi-South, J. (2020). Genomic analyses reveal three independent introductions of the invasive brown rat (*Rattus norvegicus*) to the Faroe Islands. Heredity *124*, 15–27.
11. Sjodin, B.M.F., Puckett, E.E., Irvine, R.L., Munshi-South, J., and Russello, M.A. (2021). Global origins of invasive brown rats (*Rattus norvegicus*) in the Haida Gwaii archipelago. Biol. Invasions *23*, 611–623.
12. Kurle, C.M., Zilliacus, K.M., Sparks, J., Curl, J., Bock, M., Buckelew, S., Williams, J.C., Wolf, C.A., Holmes, N.D., Plissner, J., et al. (2021). Indirect effects of invasive rat removal result in recovery of island rocky intertidal community structure. Sci. Rep. *11*, 5395.
13. Wang, S., Deng, T., Zhang, J., and Li, Y. (2023). Global economic costs of mammal invasions. Sci. Total Environ. *857*, 159479.
14. Parker, I.M., Rodriguez, J., and Loik, M.E. (2003). An evolutionary approach to understanding the biology of invasions: Local adaptation and general-purpose genotypes in the weed *Verbascum thapsus*. Conserv. Biol. *17*, 59–72.
15. Moore, M.P., Hersch, K., Sricharoen, C., Lee, S., Reice, C., Rice, P., Kronick, S., Medley, K.A., and Fowler-Finn, K.D. (2021). Sex-specific ornament evolution is a consistent feature of climatic adaptation across space and time in dragonflies *118*, e2101458118.
16. Parker, D.J., Envall, T., Ritchie, M.G., and Kankare, M. (2021). Sex-specific responses to cold in a very cold-tolerant, northern Drosophila species. Heredity *126*, 695–705.
17. Kawecki, T.J., and Ebert, D. (2004). Conceptual issues in local adaptation. Ecol. Lett. *7*, 1225–1241.
18. Colautti, R.I., and Lau, J.A. (2015). Contemporary evolution during invasion: evidence for differentiation, natural selection, and local adaptation. Mol. Ecol. *24*, 1999–2017.
19. Sears, M.W., and Angilletta, M.J., Jr. (2011). Introduction to the symposium: Responses of organisms to climate change: A synthetic approach to the role of thermal adaptation. Integr. Comp. Biol. *51*, 662–665.
20. Van Petegem, K.H.P., Boeye, J., Stoks, R., and Bonte, D. (2016). Spatial selection and local adaptation jointly shape life-history evolution during range expansion. Am. Nat. *188*, 485–498.
21. Li, Y., Tian, X., Sui, C.G., Jiang, Y.H., Liu, Y.P., Meng, F.D., and Yan, S. (2016). Climate and topography explain range sizes of terrestrial vertebrates. Nat. Clim. Change *82*, 498–508.
22. Morgan, K., Mboumba, J.F., Ntie, S., Mickala, P., Miller, C.A., Zhen, Y., Harrigan, R.J., Le Underwood, V., Ruegg, K., Fokam, E.B., et al. (2020). Precipitation and vegetation shape patterns of genomic and craniometric variation in the central African rodent *Praomys misonnei*. Proc. Biol. Sci. *287*, 20200449.
23. Keller, I., and Seehausen, O. (2012). Thermal adaptation and ecological speciation. Mol. Ecol. *21*, 782–799.
24. Wiberg, R.A.W., Tyukmaeva, V., Hoikkala, A., Ritchie, M.G., and Kankare, M. (2021). Cold adaptation drives population genomic divergence in the ecological specialist, *Drosophila montana*. Mol. Ecol. *30*, 3783–3796.
25. Teske, P.R., Sandoval-Castillo, J., Golla, T.R., Emami-Khoyi, A., Tine, M., von der Heyden, S., and Beheregaray, L.B. (2019). Thermal selection as a driver of marine ecological speciation. Proc. Biol. Sci. *286*, 20182023.
26. Key, F.M., Abdul-Aziz, M.A., Mundry, R., Peter, B.M., Sekar, A., D'Amato, M., Dennis, M.Y., Schmidt, J.M., and Andrés, A.M. (2018). Human local adaptation of the TRPM8 cold receptor along a latitudinal cline. PLoS Genet. *14*, e1007298.
27. Schluter, D. (2016). Speciation, ecological opportunity, and latitude. Am. Nat. *187*, 1–18.
28. Weir, J.T., and Schluter, D. (2007). The latitudinal gradient in recent speciation and extinction rates of birds and mammals. Science *315*, 1574–1576.
29. Delph, L.F. (2018). The Study of Local Adaptation: A Thriving Field of Research. J. Hered. *109*, 1–2.
30. Berger, J., Hartway, C., Gruzdev, A., and Johnson, M. (2018). Climate degradation and extreme icing events constrain life in cold-adapted mammals. Sci. Rep. *8*, 1156.
31. Deb, J.C., Forbes, G., and MacLean, D.A. (2020). Modelling the spatial distribution of selected North American woodland mammals under future climate scenarios. Mamm Rev. *50*, 440–452.
32. Sax, D.F., Stachowicz, J.J., Brown, J.H., Bruno, J.F., Dawson, M.N., Gaines, S.D., Grosberg, R.K., HastingS, A., Holt, R.D., Mayfield, M.M., et al. (2007). Ecological and evolutionary insights from species invasions. Trends Ecol. Evol. *22*, 465–471.
33. Mensch, J., Kreiman, L., Schilman, P.E., Hasson, E., Renault, D., and Colinet, H. (2021). Divergent metabolomic profiles of cold-exposed mature and immature females of tropical versus temperate Drosophila species. Comp. Biochem. Physiol. Mol. Integr. Physiol. *258*, 110995.
34. Chen, Y., Hou, G., Jing, M., Teng, H., Liu, Q., Yang, X., Wang, Y., Qu, J., Shi, C., Lu, L., et al. (2021). Genomic analysis unveils mechanisms of northward invasion and signatures of plateau adaptation in the Asian house rat. Mol. Ecol. *30*, 6596–6610.
35. Lagos, M.E., White, C.R., and Marshall, D.J. (2017). Do invasive species live faster? Mass-specific metabolic rate depends on growth form and invasion status. Funct. Ecol. *31*, 2080–2086.
36. Servedio, M.R., and Boughman, J.W. (2017). The role of sexual selection in local adaptation and speciation. In Annual Review of Ecology, Evolution, and Systematics, D.J. Futuyma, ed., pp. 85–109.
37. Malacrinò, A., Kimber, C.M., Brengdahl, M., and Friberg, U. (2019). Heightened condition-dependence of the sexual transcriptome as a function of genetic quality in Drosophila melanogaster head tissue. Proc. Biol. Sci. *286*, 20190819.
38. Cardoso, G.C., Batalha, H.R., Reis, S., and Lopes, R.J. (2014). Increasing sexual ornamentation during a biological invasion. Behav. Ecol. *25*, 916–923.
39. Brennan, P.A., and Zufall, F. (2006). Pheromonal communication in vertebrates. Nature *444*, 308–315.
40. Zhang, Y.H., and Zhang, J.X. (2014). A male pheromone-mediated trade-off between female preferences for genetic compatibility and sexual attractiveness in rats. Front. Zool. *11*, 73.
41. Kumar, V., Vasudevan, A., Soh, L.J.T., Le Min, C., Vyas, A., Zewail-Foote, M., and Guarraci, F.A. (2014). Sexual attractiveness in male rats is associated with greater concentration of major urinary proteins. Biol. Reprod. *91*, 150.
42. Zhu, M., Xu, X., Li, Y., Wang, P., Niu, S., Zhang, K., and Huang, X. (2019). Biosynthesis of the nematode attractant 2-heptanone and its co-evolution between the pathogenic bacterium *Bacillus nematocida* and non-pathogenic bacterium *Bacillus subtilis*. Front. Microbiol. *10*, 1489.
43. Hui, X., Zhu, W., Wang, Y., Lam, K.S.L., Zhang, J., Wu, D., Kraegen, E.W., Li, Y., and Xu, A. (2009). Major urinary protein-1 increases energy expenditure and improves glucose intolerance through enhancing mitochondrial function in skeletal muscle of diabetic mice. J. Biol. Chem. *284*, 14050–14057.
44. Zhou, Y., Jiang, L., and Rui, L. (2009). Identification of mup1 as a regulator for glucose and lipid metabolism in mice. J. Biol. Chem. *284*, 11152–11159.
45. Zhou, Y., and Rui, L. (2010). Major urinary protein regulation of chemical communication and nutrient metabolism. Vitam. Horm. *83*, 151–163.
46. Portet, R. (1981). Lipid biochemistry in the cold-acclimated rat. Comp. Biochem. Physiol. B Biochem. Mol. Biol. *70*, 679–688.
47. Lee, S.H., Dobrzyn, A., Dobrzyn, P., Rahman, S.M., Miyazaki, M., and Ntambi, J.M. (2004). Lack of stearoyl-CoA desaturase 1 upregulates basal thermogenesis but causes hypothermia in a cold environment. J. Lipid Res. *45*, 1674–1682.
48. Zou, Y., Wang, Y.N., Ma, H., He, Z.H., Tang, Y., Guo, L., Liu, Y., Ding, M., Qian, S.W., and Tang, Q.Q. (2020). SCD1 promotes lipid mobilization in subcutaneous white adipose tissue. J. Lipid Res. *61*, 1589–1604.
49. Zeng, L., Ming, C., Li, Y., Su, L.Y., Su, Y.H., Otecko, N.O., Dalecky, A., Donnellan, S., Aplin, K., Liu, X.H., et al. (2018). Out of southern east asia of the brown rat revealed by large-scale genome sequencing. Mol. Biol. Evol. *35*, 149–158.
50. Teng, H., Zhang, Y., Shi, C., Mao, F., Cai, W., Lu, L., Zhao, F., Sun, Z., and Zhang, J. (2017). Population genomics reveals speciation and introgression between brown norway rats and their sibling species. Mol. Biol. Evol. *34*, 2214–2228.
51. Deinum, E.E., Halligan, D.L., Ness, R.W., Zhang, Y.H., Cong, L., Zhang, J.X., and Keightley, P.D. (2015). Recent evolution in *Rattus norvegicus* is shaped by declining effective population size. Mol. Biol. Evol. *32*, 2547–2558.
52. Combs, M., Byers, K.A., Ghersi, B.M., Blum, M.J., Caccone, A., Costa, F., Himsworth, C.G., Richardson, J.L., and Munshi-South, J. (2018). Urban rat races: spatial population

genomics of brown rats (*Rattus norvegicus*) compared across multiple cities. Proc. Biol. Sci. *285*, 20180245.
53. Gardner-Santana, L.C., Norris, D.E., Fornadel, C.M., Hinson, E.R., Klein, S.L., and Glass, G.E. (2009). Commensal ecology, urban landscapes, and their influence on the genetic characteristics of city-dwelling Norway rats (*Rattus norvegicus*). Mol. Ecol. *18*, 2766–2778.
54. Combs, M., Puckett, E.E., Richardson, J., Mims, D., and Munshi-South, J. (2018). Spatial population genomics of the brown rat (*Rattus norvegicus*) in New York City. Mol. Ecol. *27*, 83–98.
55. Wang, Y.X. (2003). A Complete Checklists of Mammal Species and Subspecies in China (China Forestry Publishing House).
56. Wu, D.L. (1982). Subspecies of the brown rat (*Rattus norvegicus Berkenhout*) in China. Acta Theriol. Sin. *2*, 107–112.
57. Howell, A.B. (1929). Mammals from China in the collections of the United States National Museum. Proc. U. S. Natl. Mus. *75*, 1–82.
58. Ellerman, J.R., and Morrison-Scott, T.C.S. (1951). Checklist of Palaearctic and Indian Mammals 1758 to 1946 (British Museum (Natural History)).
59. Rice, A.M., Rudh, A., Ellegren, H., and Qvarnström, A. (2011). A guide to the genomics of ecological speciation in natural animal populations. Ecol. Lett. *14*, 9–18.
60. Dowle, E.J., Morgan-Richards, M., and Trewick, S.A. (2013). Molecular evolution and the latitudinal biodiversity gradient. Heredity *110*, 501–510.
61. Zhang, Y.H., Zhao, L., Fu, S.H., Wang, Z.S., and Zhang, J.X. (2021). Male pheromones and their reception by females are co-adapted to affect mating success in two subspecies of brown rats. Curr. Zool. *67*, 371–382.
62. Nigenda-Morales, S.F., Harrigan, R.J., and Wayne, R.K. (2018). Playing by the rules? Phenotypic adaptation to temperate environments in an American marsupial. PeerJ *6*, e4512.
63. Alexander, D.H., Novembre, J., and Lange, K. (2009). Fast model-based estimation of ancestry in unrelated individuals. Genome Res. *19*, 1655–1664.
64. Caye, K., Deist, T.M., Martins, H., Michel, O., and François, O. (2016). TESS3: fast inference of spatial population structure and genome scans for selection. Mol. Ecol. Resour. *16*, 540–548.
65. Lawson, D.J., Hellenthal, G., Myers, S., and Falush, D. (2012). Inference of population structure using dense haplotype data. PLoS Genet. *8*, e1002453.
66. Pickrell, J.K., and Pritchard, J.K. (2012). Inference of population splits and mixtures from genome-wide allele frequency data. PLoS Genet. *8*, e1002967.
67. Gronau, I., Hubisz, M.J., Gulko, B., Danko, C.G., and Siepel, A. (2011). Bayesian inference of ancient human demography from individual genome sequences. Nat. Genet. *43*, 1031–1034.
68. Liu, X., and Fu, Y.-X. (2020). Stairway Plot 2: demographic history inference with folded SNP frequency spectra. Genome Biol. *21*, 280.
69. Excoffier, L., Dupanloup, I., Huerta-Sánchez, E., Sousa, V.C., and Foll, M. (2013). Robust demographic inference from genomic and SNP data. PLoS Genet. *9*, e1003905.
70. Derryberry, E.P., Derryberry, G.E., Maley, J.M., and Brumfield, R.T. (2014). hzar: hybrid zone analysis using an R software package. Mol. Ecol. Resour. *14*, 652–663.
71. Gompert, Z., and Alex Buerkle, C. (2010). INTROGRESS: a software package for mapping components of isolation in hybrids. Mol. Ecol. Resour. *10*, 378–384.
72. Zhao, L., Zhang, J.X., and Zhang, Y.H. (2020). Genetic boundary and gene flow between 2 parapatric subspecies of brown rats. Curr. Zool. *66*, 677–688.
73. Taylor, S.A., Larson, E.L., and Harrison, R.G. (2015). Hybrid zones: windows on climate change. Trends Ecol. Evol. *30*, 398–406.
74. Edmonds, R.L. (1979). The willow palisade. Ann. Assoc. Am. Geogr. *69*, 599–621.
75. Jia, D., Li, Y., and Fang, X. (2018). Complexity of factors influencing the spatiotemporal distribution of archaeological settlements in northeast China over the past millennium. Quat. Res. *89*, 413–424.
76. Johnson, M.T.J., and Munshi-South, J. (2017). Evolution of life in urban environments. Science *358*, eaam8327.
77. Martinez Barrio, A., Lamichhaney, S., Fan, G., Rafati, N., Pettersson, M., Zhang, H., Dainat, J., Ekman, D., Höppner, M., Jern, P., et al. (2016). The genetic basis for ecological adaptation of the Atlantic herring revealed by genome sequencing. Elife *5*, e12081.
78. Beckman, E.J., Martins, F., Suzuki, T.A., Bi, K., Keeble, S., Good, J.M., Chavez, A.S., Ballinger, M.A., Agwamba, K., and Nachman, M.W. (2022). The genomic basis of high-elevation adaptation in wild house mice (*Mus musculus domesticus*) from South America. Genetics *220*, iyab226.
79. Ferris, K.G., Chavez, A.S., Suzuki, T.A., Beckman, E.J., Phifer-Rixey, M., Bi, K., and Nachman, M.W. (2021). The genomics of rapid climatic adaptation and parallel evolution in North American house mice. PLoS Genet. *17*, e1009495.
80. Abumrad, N.A. (2017). The liver as a hub in thermogenesis. Cell Metab. *26*, 454–455.
81. Teeter, K.C., Payseur, B.A., Harris, L.W., Bakewell, M.A., Thibodeau, L.M., O'Brien, J.E., Krenz, J.G., Sans-Fuentes, M.A., Nachman, M.W., and Tucker, P.K. (2008). Genome-wide patterns of gene flow across a house mouse hybrid zone. Genome Res. *18*, 67–76.
82. Wilson, A.G., Wilson, S., Alavi, N., and Lapen, D.R. (2021). Human density is associated with the increased prevalence of a generalist zoonotic parasite in mammalian wildlife. Proc. Biol. Sci. *288*, 20211724.
83. Lee, K.A., and Klasing, K.C. (2004). A role for immunology in invasion biology. Trends Ecol. Evol. *19*, 523–529.
84. Janoušek, V., Munclinger, P., Wang, L., Teeter, K.C., and Tucker, P.K. (2015). Functional organization of the genome may shape the species boundary in the house mouse. Mol. Biol. Evol. *32*, 1208–1220.
85. Yu, X.X., Lewin, D.A., Forrest, W., and Adams, S.H. (2002). Cold elicits the simultaneous induction of fatty acid synthesis and β-oxidation in murine brown adipose tissue: prediction from differential gene expression and confirmation in vivo. FASEB J *16*, 155–168.
86. ALjohani, A.M., Syed, D.N., and Ntambi, J.M. (2017). Insights into stearoyl-CoA desaturase-1 regulation of systemic metabolism. Trends Endocrinol. Metab. *28*, 831–842.
87. Zhang, Y.H., Zhao, L., Guo, X., Zhang, J.H., and Zhang, J.X. (2019). Sex pheromone levels are associated with paternity rate in brown rats. Behav. Ecol. Sociobiol. *73*, 15.
88. Roberts, S.C., and Gosling, L.M. (2003). Genetic similarity and quality interact in mate choice decisions by female mice. Nat. Genet. *35*, 103–106.
89. Andersson, M., and Simmons, L.W. (2006). Sexual selection and mate choice. Trends Ecol. Evol. *21*, 296–302.
90. Lounsbury, A.C. (2014). The role of body size on the outcome of mating interactions in *Drosophila melanogaster*. Master of Science (Wilfrid Laurier University).
91. Gómez-Llano, M., Scott, E., and Svensson, E.I. (2021). The importance of pre- and postcopulatory sexual selection promoting adaptation to increasing temperatures. Curr. Zool. *67*, 321–327.
92. Smadja, C., Catalan, J., and Ganem, G. (2003). Strong premating divergence in a unimodal hybrid zone between two subspecies of the house mouse. J. Evol. Biol. *17*, 165–176.
93. Mihola, O., Trachtulec, Z., Vlcek, C., Schimenti, J.C., and Forejt, J. (2009). A mouse speciation gene encodes a meiotic histone H3 methyltransferase. Science *323*, 373–375.
94. Carneiro, M., Albert, F.W., Afonso, S., Pereira, R.J., Burbano, H., Campos, R., Melo-Ferreira, J., Blanco-Aguiar, J.A., Villafuerte, R., Nachman, M.W., et al. (2014). The genomic architecture of population divergence between subspecies of the European rabbit. PLoS Genet. *10*, e1003519.
95. Teng, H., Zhang, Y., Shi, C., Mao, F., Hou, L., Guo, H., Sun, Z., and Zhang, J. (2016). Whole-genome sequencing reveals genetic variation in the asian house rat. G3 (Bethesda). *6*, 1969–1977.
96. Chen, Y., Zhao, L., Teng, H., Shi, C., Liu, Q., Zhang, J., and Zhang, Y. (2021). Population genomics reveal rapid genetic differentiation in a recently invasive population of *Rattus norvegicus*. Front. Zool. *18*, 6.
97. Fick, S.E., and Hijmans, R.J. (2017). WorldClim 2: new 1-km spatial resolution climate surfaces for global land areas. Int. J. Climatol. *37*, 4302–4315.
98. Li, H., and Durbin, R. (2009). Fast and accurate short read alignment with Burrows-Wheeler transform. Bioinformatics *25*, 1754–1760.
99. McKenna, A., Hanna, M., Banks, E., Sivachenko, A., Cibulskis, K., Kernytsky, A., Garimella, K., Altshuler, D., Gabriel, S., Daly, M., et al. (2010). The genome analysis toolkit: a mapreduce framework for analyzing next-generation DNA sequencing data. Genome Res. *20*, 1297–1303.
100. Danecek, P., Auton, A., Abecasis, G., Albers, C.A., Banks, E., Depristo, M.A., Handsaker, R.E., Lunter, G., Marth, G.T., Sherry, S.T., et al. (2011). The variant call format and VCFtools. Bioinformatics *27*, 2156–2158.
101. Lischer, H.E.L., and Excoffier, L. (2012). PGDSpider: an automated data conversion tool for connecting population genetics and genomics programs. Bioinformatics *28*, 298–299.
102. Excoffier, L., and Lischer, H.E.L. (2010). Arlequin suite ver 3.5: a new series of programs to perform population genetics analyses under Linux and Windows. Mol. Ecol. Resour. *10*, 564–567.
103. McRae, B.H., Dickson, B.G., Keitt, T.H., and Shah, V.B. (2008). Using circuit theory to

model connectivity in ecology, evolution, and conservation. Ecology *89*, 2712–2724.
104. Szpiech, Z.A., and Hernandez, R.D. (2014). Selscan: an efficient multithreaded program to perform ehh-based scans for positive selection. Mol. Biol. Evol. *31*, 2824–2827.
105. Dobin, A., Davis, C.A., Schlesinger, F., Drenkow, J., Zaleski, C., Jha, S., Batut, P., Chaisson, M., and Gingeras, T.R. (2013). STAR: ultrafast universal RNA-seq aligner. Bioinformatics *29*, 15–21.
106. Jombart, T., and Ahmed, I. (2011). adegenet 1.3-1: new tools for the analysis of genome-wide SNP data. Bioinformatics *27*, 3070–3071.
107. Hijmans, R.J. (2020). Geographic Data Analysis and Modeling [R Package Raster Version 3.4-5].
108. Yu, G. (2020). Gene ontology semantic similarity analysis using GOSemSim. In Stem Cell Transcriptional Networks: Methods and Protocols, B.L. Kidder, ed. (Springer US), pp. 207–215.
109. Wu, T., Hu, E., Xu, S., Chen, M., Guo, P., Dai, Z., Feng, T., Zhou, L., Tang, W., Zhan, L., et al. (2021). clusterProfiler 4.0: A universal enrichment tool for interpreting omics data. Innovation *2*, 100141.
110. Oksanen, J., Blanchet, F.G., Kindt, R., Legendre, P., Minchin, P., O'hara, R., Simpson, G., Solymos, P., Stevens, M., and Wagner, H. (2017). Vegan: community ecology package [R package Vegan version 2.5].
111. Luu, K., Bazin, E., and Blum, M.G.B. (2017). pcadapt: anRpackage to perform genome scans for selection based on principal component analysis. Mol. Ecol. Resour. *17*, 67–77.
112. Love, M.I., Huber, W., and Anders, S. (2014). Moderated estimation of fold change and dispersion for RNA-seq data with DESeq2. Genome Biol. *15*, 550.
113. Wang, I.J. (2013). Examining the full effects of landscape heterogeneity on spatial genetic variation: a multiple matrix regression approach for quantifying geographic and ecological isolation. Evolution *67*, 3403–3411.
114. Xie, C., Yuan, J., Li, H., Li, M., Zhao, G., Bu, D., Zhu, W., Wu, W., Chen, R., and Zhao, Y. (2014). NONCODEv4: exploring the world of long non-coding RNA genes. Nucleic Acids Res. *42*, D98–D103.
115. Rambaut, A., Drummond, A.J., Xie, D., Baele, G., and Suchard, M.A. (2018). Posterior summarization in Bayesian phylogenetics using tracer 1.7. Syst. Biol. *67*, 901–904.
116. Akaike, H. (1974). A New Look at the Statistical Model Identification. IEEE Trans. Automat. Control *19*, 716–723.
117. Meredith, M., and Kruschke, J. (2018). HDInterval: Highest (Posterior) Density Intervals [R Package HDInterval version 0.1.3.
118. Chen, J., Chen, J., Liao, A., Cao, X., Chen, L., Chen, X., He, C., Han, G., Peng, S., Lu, M., et al. (2015). Global land cover mapping at 30m resolution: A POK-based operational approach. ISPRS J. Photogrammetry Remote Sens. *103*, 7–27.
119. SEDAC (2020). Gridded Population of the World, Version 4 (GPWv4): Population Density, Revision 11. https://sedac.ciesin.columbia.edu/data/set/gpw-v4-population-density-rev11.
120. Balkenhol, N., Dudaniec, R.Y., Krutovsky, K.V., Johnson, J.S., Cairns, D.M., Segelbacher, G., Selkoe, K.A., von der Heyden, S., Wang, I.J., Selmoni, O., et al. (2017). Landscape Genomics: Understanding Relationships Between Environmental Heterogeneity and Genomic Characteristics of Populations. In Population Genomics: Concepts, Approaches and Applications, O.P. Rajora, ed. (Springer International Publishing)), pp. 261–322.
121. Ersts, P. (2019). Geographic Distance Matrix Generator Version 1.23. http://biodiversityinformatics.amnh.org/open_source/gdng.
122. Smouse, P.E., Long, J.C., and Sokal, R.R. (1986). Multiple regression and correlation extensions of the Mantel test of matrix correspondence. Syst. Zool. *35*, 627–632.
123. Kolberg, L., Raudvere, U., Kuzmin, I., Vilo, J., and Peterson, H. (2020). gprofiler2 – an R package for gene list functional enrichment analysis and namespace conversion toolset g:Profiler. F1000Res. *9*, 709.

STAR★METHODS

KEY RESOURCES TABLE

REAGENT or RESOURCE	SOURCE	IDENTIFIER
Deposited data		
Raw sequencing data	This paper	SRA:PRJNA825662
Raw sequencing data	Deinum et al.[51]	ENA:ERP001276
Raw sequencing data	Teng et al.[95]	SRA:SRX1425877 SRA:SRX1425879
Raw sequencing data	Teng et al.[50]	SRA:SRP078989
Raw sequencing data	Chen et al.[96]	GSA:CRA001635
Rat reference genome Rnor_5.0	Rat Genome Sequencing Consortium	https://www.ncbi.nlm.nih.gov/assembly/GCF_000001895.4
Rat reference genome Rnor_6.0	Rat Genome Sequencing Consortium	https://www.ncbi.nlm.nih.gov/assembly/GCA_000001895.4
WorldClim	Fick & Hijmans [97]	http://www.worldclim.com/version2
GlobeLand30	Global Change Research Data Publishing & Repository	http://www.geodoi.ac.cn/WebCn/doi.aspx?Id=163
Crop yield	the Resource and Environment Science Data Center of the Chinese Academy of Sciences	http://www.resdc.cn
Population density	Socioeconomic Data and Applications Center	https://sedac.ciesin.columbia.edu/
Software and algorithms		
BWA v0.7.9a	Li & Durbin [98]	http://bio-bwa.sourceforge.net/
GATK v4.2.5	McKenna et al.[99]	https://gatk.broadinstitute.org/hc/en-us
SAMtools v0.0.19	Li et al.[98]	http://samtools.github.io/
VCFtools v0.1.13	Danecek et al.[100]	https://github.com/vcftools/vcftools
ADMIXTURE v1.3	Alexander, Novembre & Lange[63]	https://dalexander.github.io/admixture/
fineSTRUCTURE v4.0.1	Lawson et al.[65]	https://people.maths.bris.ac.uk/~madjl/finestructure/finestructure_info.html
TREEMIX v1.12	Pickrell & Pritchard[66]	https://bitbucket.org/nygcresearch/treemix/wiki/Home
G-PhoCS v1.2.3	Gronau et al.[67]	http://compgen.cshl.edu/GPhoCS/
Stairway Plot v2	Liu & Fu[68]	https://github.com/xiaoming-liu/stairway-plot-v22
fastsimcoal2 v2.6	Excoffier et al.[69]	http://cmpg.unibe.ch/software/fastsimcoal26/
easySFS	https://github.com/isaacovercast/easySFS#easysfs	https://github.com/isaacovercast/easySFS#easysfs
PGDSpider v2.1.1.3	Lischer & Excoffier[101]	http://cmpg.unibe.ch/software/PGDSpider/
Arlequin v3.5	Excoffier & Lischer[102]	http://cmpg.unibe.ch/software/arlequin3/
ArcMap v10.5	ESRI, Redlands, CA, USA	www.arcgis.com
Circuitscape v4.0.3	McRae et al.[103]	https://circuitscape.org/
selscan v1.3.0	Szpiech & Hernandez[104]	https://github.com/szpiech/selscan
STARv2.7.9a	Dobin et al.[105]	http://code.google.com/p/rna-star/
tess3r	Caye et al.[64]	https://cran.r-project.org/src/contrib/Archive/tess3r/
adegenet v2.0.1	Jombart & Ahmed[106]	https://cran.r-project.org/src/contrib/Archive/adegenet/

(*Continued on next page*)

Continued

REAGENT or RESOURCE	SOURCE	IDENTIFIER
raster v3.4.5	Hijmans[107]	https://cran.r-project.org/src/contrib/Archive/raster/
HZAR v0.2-5	Derryberry et al.[70]	https://cran.r-project.org/src/contrib/Archive/hzar/
introgress v1.2.3	Gompert & Buerkle [71]	https://cran.r-project.org/src/contrib/Archive/introgress/
clusterProfiler v4.0	Yu[108]; Wu et al.[109]	https://bioconductor.org/packages/release/bioc/html/clusterProfiler.html
GOSemSim v2.22.0	Yu[108]	https://bioconductor.org/packages/release/bioc/html/GOSemSim.html
vegan v2.5	Oksanen et al.[110]	https://cran.r-project.org/src/contrib/Archive/vegan/
pcadapt v4.3.2	Luu, Bazin & Blum [111]	https://cran.r-project.org/src/contrib/Archive/pcadapt/
DESeq2 v1.24.0	Love, Huber & Anders [112]	https://bioconductor.org/packages/release/bioc/html/DESeq2.html
MMRR	Wang [113]	https://datadryad.org/stash/dataset/doi:10.5061/dryad.kt71r

RESOURCE AVAILABILITY

Lead contact

Further information and requests for resources and reagents should be directed to and will be fulfilled by the lead contact, Jian-Xu Zhang (zhangjx@ioz.ac.cn or zhangjx.rat@outlook.com).

Materials availability

This study did not generate new unique reagents.

Data and code availability

- The raw sequence data generated in this paper have been deposited at GenBank Sequence Read Archive (SRA) and are publicly available as of the date of publication. Accession numbers are listed in the key resources table.
- This paper does not report original code.
- Any additional information required to reanalyze the data reported in this work paper is available from the lead contact upon request.

EXPERIMENTAL MODEL AND STUDY PARTICIPANT DETAILS

We analyzed WGSs of 48 *R norvegicus* individuals distributed over 1,100 km in northern and NE China from Harbin (HB) (the center of the RNC range) to Beijing (BJ) (the center of the RNC range) and two individuals of *R. rattus* and *R. tanezumi* as an outgroup. Among these samples, 34 were previously sequenced,[50,51,95,96] and 16 *R norvegicus* sequences were newly generated (Figure 1A; Table S1).

We randomly selected one-year-old RNH and RNC rats from outbred colonies of approximately 300–400 individuals of each subspecies. The ancestors of these captive-bred rats were captured alive in rural areas of Beijing and Harbin, respectively. They were maintained in our laboratory (14-h light:10-h dark cycle, 23 ± 2°C). Six one-year-old males and females of each subspecies were used for MUPs and hepatic transcriptome analysis, 12 males for temperature acclimation, and 32 males and 16 females for mate choice tests.

Ethics approval

All procedures for animal care and use were performed in strict accordance with the ethical standards of the institutional research committee. Ethical approval (IOZ2017 06) was obtained from the Ethical Committees of the Institute of Zoology, Chinese Academy of Sciences.

METHOD DETAILS

Samples, DNA extraction, library preparation, and variant calling

We extracted DNA, constructed libraries and sequenced them at 2 × 150 bp on an Illumina HiSeq X Ten instrument (Illumina Inc., CA, USA). We filtered the raw reads and aligned them using BWA v0.7.9a.[98] We aligned 32 individuals with known geographic coordinates of sampling

sites to the Rnor_5.0 reference genome (mean depth 10.22–23.92) and detected SNPs using GATK HaplotypeCaller v3.2.2 and Samtools mpileup v0.0.19 with best practice recommendations or default parameters.[50,99] We also aligned all 50 samples to Rnor_6.0 and detected SNPs using GATK HaplotypeCaller v4.2.5 and filtered with default parameters (Table S1). We further used VCFtools v0.1.13[100] to keep the biallelic variants and remove sites with a minor allele frequency (MAF) < 0.05 and sites where at least 10% of individuals lacked calls.[34,49]

Population structure analysis

We pruned SNPs under linkage disequilibrium with a correlation coefficient greater than 0.1 and performed PCA and sPCA using the R package adegenet v2.0.1.[106] We also ran ADMIXTURE v1.3 [63] and ran TESS3 with the R package tess3r.[64] We phased and converted the SNPs to CHROMOPAINTER format to further explore population structure using fineSTRUCTURE v4.0.1.[65] We ran TREEMIX v1.12 with 0–2 migration events and blocks of 500 SNPs, and we set *R. rattus* and *R. tanezumi* as the outgroup and evaluated the models by considering both the residuals and the proportion of variance explained.[66]

Demographic history

We applied Generalized Phylogenetic Coalescent Sampler (G-PhoCS) v1.2.3[67] to infer the demographic history of the RNH and RNC core populations.[50] We selected 4,542 autosomal neutral loci with a length of 1 kb, an inter-locus distance of more than 50 kb, a mean PhastCons score less than 0.5 and a distance of at least 100 kb from a gene. We excluded loci containing the following elements: protein-coding DNA, expressed sequence tags (ESTs), LincRNA (NONCODEv4),[114] N's, repeat-masked sequences, simple repeat sequences and segmental duplications. We ran Markov chain Monte Carlo (MCMC) algorithms for 1,000,000 iterations with the first 10% iterations as burn-in and evaluated the convergence by Tracer v1.6[50,115]. We used a mutation rate of 9.29×10^{-8} per site per generation[5] and a generation time of 0.5 years[50] We converted the divergence time (τ) into years with the equation $T = \tau/\mu$ and estimated Ne as $\theta/(4\times\mu)$.

The G-PhoCS approach cannot be used to infer changes in Ne over time, and the gene flow inferred by G-PhoCS was inconsistent across replicates. We additionally performed site frequency spectrum (SFS)-based methods with Stairway Plot v2[68] and fastsimcoal2 v2.6.[69] To construct the SFS, we prepared a VCF file by using non-transcribed regions with no MAF threshold and polarized the variants to ancestral and derived alleles based on the outgroup (*R. rattus* and *R. tanezumi*) sequences.[5,49] For the Stairway Plot analysis, we generated the SFS of non-transcribed regions at least 50 kb away from coding regions with easySFS (https://github.com/isaacovercast/easySFS#easysfs). We ran four iterations, each with a different number of random breakpoints that corresponded to the sample size, and accepted the best model based on the composite likelihood. We created 200 input files and estimated the medians and 95% confidence intervals of demographic parameters. For fastsimcoal2 analysis, we filtered out the SNPs located within 10 kb of coding regions, took one SNP every 10 kb, and generated the joint SFS with PGDSpider v2.1.1.3 and Arlequin v3.5[101,102]. The times of divergence and bottlenecks and the search ranges were set by the parameters inferred from G-PhoCS and Stairway Plot. We generated five models for fastsimcoal2: isolation-only (IO), isolation-with-migration (IM), IM-and-bottleneck (IMB), isolation-with-secondary contact (SC) and IMB-with-secondary contact (IMBSC) models. We ran each model 400 times with the parameters -n 100000 -L 40 and selected the best model using the maximum likelihood value and Akaike information criterion (AIC).[116] With the best model, we generated 300 samples of pairwise SFS algorithms, each containing 100,000 sites to estimate parameter ranges, and calculated the 90% highest posterior density using the HDInterval v0.1.3 R package.[5,49,117]

Testing the influence of landscape on gene flow

We obtained 19 bioclimatic variables and digital elevation with a resolution of 30 arc-seconds (~1 km) from the WorldClim database.[97] We also obtained land cover data from the GlobeLand30 database,[118] crop yield data from the Resource and Environment Science Data Center of the Chinese Academy of Sciences (http://www.resdc.cn) and population density data from the Socioeconomic Data and Applications Center.[119]

First, we related the genetic distances between sampling sites to between-site landscape factors. We evaluated the following models: isolation-by-distance (IBD), isolation-by-environment (IBE), isolation-by-resistance (IBR), and isolation-by-barrier (IBB) models. IBD and IBE predict that genetic distance increases with geographic distance and environmental differences, while IBR reflects the ecological or physiological limitation of dispersal, and IBB occurs when strong migration barriers sharply reduce gene flow.[120] For the IBE models, we generated a distance matrix with Geographic distance matrix generator v1.2.3,[121] extracted the values of the variables for each sampling point using the R package raster v3.4.5,[107] transformed the climate variables using PCA, and estimated the genetic distance and the environmental distance with the R package adegenet v2.1.2.[106] For the IBR models, we generated five resistance maps and calculated the resistance distances between each pair of sample sites: (1) a null IBD map (all cells were given a resistance value of 1); (2) a topography map based on the slope calculated from elevation; (3) a land cover map (cultivated land, bare land, and artificial surfaces were given a resistance value of 1; forest, grassland, shrubland: 20; wetland: 30; water bodies, permanent snow and ice: 100); (4) a crop yield map; and (5) a human population map. Each map was compiled on a separate raster grid with a resolution of 1 km in ArcMap v10.5 (ESRI, Redlands, CA, USA). We transformed the resistance maps into resistance distance matrices with Circuitscape v4.0.3.[103] We also tested an IBB model, where the distance equaled 1 if the samples were on the same side of the Shanhai Pass and 0 otherwise. We conducted Mantel tests and multiple matrix regression with randomization (MMRR) analysis to examine the effects of IBD, IBE, IBR, and IBB on genetic distance.[122,113] We performed (1) simple Mantel tests between the genetic distance matrix and each of the geographic, environmental, resistance and barrier distance matrices, (2) partial Mantel tests between the genetic distance matrix and a second matrix while controlling for the effects of a third matrix, and (3) MMRR as

an alternative to partial Mantel tests to examine the relative contributions of the second and third distance matrices to genetic differentiation. We ran Mantel tests using the R package vegan v2.5[110] and performed both the Mantel tests and MMRR analysis using R v3.6.0.

Second, we related the genetic variance to local environmental variables at each sampling site using RDA in the R package vegan v2.5.[110] To avoid nonindependence between variables, we removed variables that showed a strong correlation ($R^2 > 0.7$) and fitted a full RDA model including all the independent environmental features. We then ran partial RDA to explore the influence of each variable. We identified the outlier SNPs (3.5 standard deviation cut-off) for each environmental variable using RDA, and we also detected outlier loci ($\alpha = 0.001$) with the R package pcadapt v4.3.2.[111]

Detection of loci under selection

We calculated the population difference (F index, F_{ST}) and nucleotide diversity (π) with VCFtools v0.1.13 in a 100-kb sliding window with a step size of 10 kb and calculated the $lg\pi_{ratio}$ as log10 (π_{RNH}/π_{RNC}). We also used selscan v1.3.0[104] to calculate XP-EHH. The outliers were determined with Z tests (significance levels of $\alpha = 0.05$ for F_{ST}, $lg\pi_{ratio}$; $\alpha = 0.0001$ for XP-EHH (score >3.90)), and the windows or the regions within 250 kb of the outlier SNPs were clustered as candidate regions. We conducted functional enrichment analysis using g:Profiler.[123] We also simulated 100,000 segments with a 100 kb window size using the parameters of the best model estimated by fastsimcoal2 and compared the FST, $lg\pi_{ratio}$ and XP-EHH values of these candidate regions with those of the simulated data.

Genomic and geographic cline analysis

We identified SNPs with fixed differences between the core populations and selected those more than 1 Mb apart as diagnostic SNPs. We conducted geographic cline analysis with the R package HZAR v0.2-5.[70] The geographic location of each sample was measured in kilometres from the northernmost locality. We also performed genomic cline analysis using the R package introgress v1.2.3.[71] We calculated the genotype-specific quantiles and examined whether each genotype was over- or underrepresented compared to neutral expectations. SNPs with a distance of less than 1 Mb were clustered as candidate regions for further annotation and enrichment analysis.

Animals used for behavioral and physiological experiments

We captured and maintained individuals of each subspecies as an outbred colony of 300–400 rats. The housing room was maintained at 23 $\pm$ 2°C and had a reversed 14:10-h light:dark photoperiod (lights on at 19:00). The female rats had a 4- and 5-day estrous cycle. The males were individually caged for 2 weeks prior to experimental use.

Temperature acclimation, hepatic MUP quantification and RNA-seq analysis

Six one-year-old males of each subspecies were randomly selected to assess subspecific differences in MUPs and hepatic gene expression. Meanwhile, 12 adult (one-year-old) males of RNH were randomly assigned to two groups for 2°C and 23°C acclimation for five consecutive days. Rats were individually caged, and acclimation was carried out in modified freezers that were ventilated by air pumps and kept at 20% O_2 and 0.05% CO_2.

We first collected urine for MUP analysis using metabolic cages, and we then euthanised the rats to collect liver tissue for transcriptome analysis. We separated the urine samples by 15% SDS–PAGE, stained the gel, and quantified the proteins using a ChemiDoc MP system (Bio-Rad, USA). For RNA-seq, we prepared 3 biological replicates for each subspecies and 4 biological replicates for the temperature-acclimated and control rats. We sequenced the libraries with the Illumina HiSeq X Ten platform, trimmed the raw reads, aligned them to the reference genome, generated read counts using STARv2.7.9a,[105] and identified the DEGs with DESeq2 v1.24.0.[112] We conducted functional enrichment analysis using g:Profiler v2 and clusterProfiler v4.0 and reduced the redundancy of GO terms using GOSemSim v2.22.0 R package.[108,109,123]

Behavioral tests of female preferences for male mates

Sixteen females for each subspecies were used as recipients in behavior tests, and 32 males for each subspecies were used as targets. Each test trio consisted of a recipient female from either the RNH or RNC subspecies and two randomly paired male RNH-RNC targets (urine scent, individuals or potential mates). The individuals in a test trio were different for each experiment, and there was a four-day interval between consecutive experiments.

We conducted preference tests in a two-choice apparatus consisting of three rat cages.[61] Two choice boxes were symmetrically connected to the long side of the start box with Plexiglas tubes. A fixed iron sheet was placed in the middle of each choice box, which divided the box into a front chamber and a rear chamber. In experiment 1 (Exp1), we allowed two RNH and RNC males to deposit urine and feces in the front chambers of choice boxes for 30 min and then moved the males away. In experiment 2 (Exp2), we placed two males in the rear chambers. For each trial in Exp1 and Exp2, we allowed a female rat to acclimate to the start box for 10 min and then allowed it to investigate the choice boxes for 30 min. We recorded the time the females spent in each of the choice boxes using EthoVision XT v15 (Noldus, Wageningen, The Netherlands). In experiment 3 (Exp3), we loosely tethered a male in each choice box and then allowed the female to freely investigate the whole apparatus. We separated the males and females until the females were obviously pregnant, and females that were not pregnant within two months were excluded from the test. After the pups were weaned, we determined paternity with microsatellite loci.[61]

QUANTIFICATION AND STATISTICAL ANALYSIS

To determine the influence of landscape on gene flow, we analyzed 40 rats with known geographic coordinates and tested the models: IBD, IBE, IBR, and IBB using Mantel tests and MMRR tests with R v3.6.0. We also related the genetic variance to local environmental variables at each sampling site using RDA in the R package vegan v2.5.[110] We identified the outlier SNPs (3.5 standard deviation cut-off) and also detected outlier loci ($\alpha = 0.001$) with the R package pcadapt v4.3.2.[111] To scan genomic regions with high differentiation between two core populations, we determined the outliers with Z tests (FST, lgπratio $p < 0.05$; XP-EHH score >3.90). To estimate the geographic and genomic clines, we performed HZAR v0.2-5[71] and introgress v1.2.3.[72] To estimate hepatic transcriptome, we randomly selected six one-year-old males of each subspecies. We determined the DEGs with DESeq2 v1.24.0,[112] log2 FoldChange >1 or < −1 and $q < 0.05$ were considered significant. We also estimated the MUP levels of these rats. We first determined the distribution of data using the Shapiro–Wilk test with SPSSv18.0. Since the raw data was normally distributed, we further compared the MUP levels using an independent *t*-test. We also used paired *t*-tests and Wilcoxon signed-rank tests for normally distributed and non-normally distributed data, respectively, in mate choice tests for 16 female subjects of each subspecies. For the above tests, $p < 0.05$ were considered significant unless otherwise stated.